Journal of the Korean Nuclear Society
Volume 15, Number 3, September, 1983

《**Original**》

The Sintering Behavior of the Hyperstoichiometric Uranium Dioxide in the Oxidative Atmosphere

Jang Keu Han and Won Ku Park
Inha University

Han Su Kim
Korea Advanced Energy Research Institute

(Received July 15, 1983)

약 산화성 분위기 중에서의 과산화성 2산화 우라늄의 소결에 관한 연구

한 장 규·박 원 구
인하대학교

김 한 수
한국에너지연구소

(1983. 7. 15 접수)

Abstract

The slightly hyperstoichiometric uranium dioxide, i.e. $UO_{2.005}$ and $UO_{2.01}$ within a range of the requirement for the use of a nuclear fuel, were sintered directly in an atmosphere of CO_2/CO mixture without any succeeding reduction process. The kinetics of sintering in the late stage were investigated for various O/U ratios. A sintering diagram, which show the relation of Temperature-Time-Density-Grain size, was established for each O/U ratio. Only by controlling the oxygen partial pressure in the sintering atmosphere, UO_2 pellet could be sintered very easily at low temperature 1050°~1200°C with a density above 95% T.D. and average grain size above 7μm. It was found that the rate of grain growth follows $D=(Kt)^{1/4}$ in the late stage of sintering. And the activation energies for grain growth in the final sintering stage were found to be 75, 64 and 62kcal/mol for $UO_{2.005}$, $UO_{2.01}$ and $UO_{2.10}$, respectively. Although no significant differences are obtained between the activation energies for different O/U ratios, the sinterability is enhanced considerably with increasing the oxygen partial pressure in the sintering atmosphere.

요 약

핵연료로서 사용 가능한 O/U비 범위인 2.005~2.01의 이산화 우라늄의 소결체를 환원 공정을 거치지 않고 직접 CO_2/CO 혼합가스 분위기에서 소결하였다. O/U비 변화가 소결속도에 미치는 영향을 소결후기에서 조사하였으며, 일정 O/U비에 있어서의 소결 온도—시간—밀도—입도 간의 관계를 나타

내는 소결 다이아그램을 결정하였다. 그결과 소결분위기중의 산소분압만을 조절하여, 이론밀도의 95 % 이상, 평균입도 7μm 이상의 소결체를 1050°~1200°C의 저온에서 쉽게 얻을 수 있었다. 소결후기의 결정입도의 성장속도는 $D=(Kt)^{1/4}$의 실험식에 따르고, 결정립성장에 대한 활성화 에너지는 O/U 비가 2.005, 2.01, 2.10일 때 각각 75, 64, 62Kal/mol이었다. O/U비가 변화해도 활성화 에너지는 크게 변하지 않았지만, 소결은 산소 분압의 증가에 따라 크게 증가하였다.

1. Introduction

The conventional technique of sintering UO_2 holds some techno-economic handicaps raising from the use of high temperature and prolonged sintering time. Hence many attempts have been made to reduce the temperature and time for sintering without affecting the qualities of sintered pellet.

Small additions of TiO_2 [1,2] or Nd_2O_3[3] accerelated the sinterability and lowered the sintering temperature to obtain a given density of pellet. However, it remains unknown whether the additives would cause a hazardous effect on irradion.

Introduction of water vapor into the furnace atmosphere enhanced significantly the rate of sintering.[4,5] Unfortunately, this method led the sintered pellets to the high O/U ratio and seperate reduction process must be followed subsequent to sintering. Moreover, the life time of refractory materials was shortened by thermal shock caused from the contact with cold steam.

W. Dörr and H. A. Assmann[6] used the CO_2 gas of the technical purity as sintering atmosphere, and could lower the sintering temperature 500°~600°C below the conventional sintering temperature. Most of the disadvantages of the steam sintering could be eliminated by introducing CO_2 as sintering atmosphere, except the subsequent reducing process.

Many attempts have been carried out to verify the sintering kinetics of UO_2 and UO_{2+x} by measuring the activation energy and the results revealed wide variation. Since most of the works were studied at the initial sintering stage,[7~11] this variation would be induced from the initial powder characteritics, green density, sintering atmosphere and temperature. Especially, the initial sintering stage would be greatly affected by the surface condition, shape and O/U ratio of the powder and the sintering atmosphere.

Furthermore, all of the sintering mechanism,[12~15] i.e. surface diffusion, grain boundary diffusion, volume diffusion etc., could be operative at a time during initial sintering stage.

The present work was intended to obtain UO_2 pellets, satisfying the nuclear specification, by a single-step-sintering at low temperature in a CO_2/CO mixed gas atmosphere, and to study the sintering kinetics and the activation energies for the oxidative sintering. To focus the problem of the study on the effects of excess oxygen in UO_2, most of the complex effects of initial sintering were eliminated by analyzing the rate of grain growth in the final sintering stage.

2. Experimental Procedure

The UO_2 powders used in this study were prepared from different processes: Powder A, prepared from ammonium uranyl carbonate,[16] Powder B, prepared from ammonium diuranate.[17] The important physical and chemical properties of these powders were listed in table 1. The particle of powder A revealed round and smooth surface, powder B, however, revealed fine irregular shape, as illustrated in SEM micrographs of fig. 1.

To eliminate the subsidiary effect of lubricant

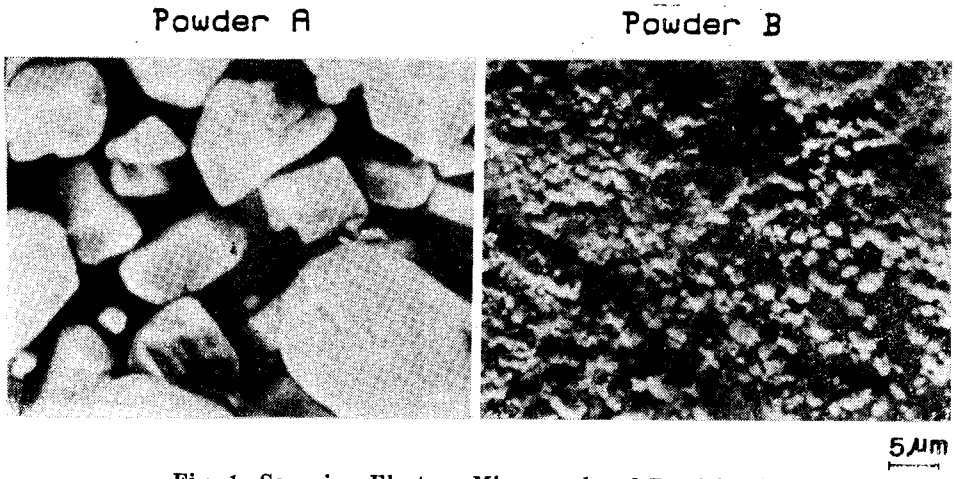

Fig, 1. Scanning Electron Micrographs of Particle Shape.

Table. 1. Physical and Chemical Properties of UO_2 Powder

Property	Powder Type	Powder A	Powder B
Enrichment U-235		0.33%	0.21%
O/U Ratio		2.15	2.05
Moisture Content	(ppm)	1001	1200
Powder Size	(μm)	7.3	0.68
Pour Density	(Mg/m^3)	2.67	1.78
Tap Density	(Mg/m^3)	2.87	2.61
Surface Rree	(m^2/g)	5.939	2.34
Powder Shape		Sphere	Irregular

during sintering, each powder was directly pressed at 3.1 ton/cm^2, without the addition of binder or lubric ant, to the green pellets of 15mm ϕ and 20mm H. Powder A could be pressed to sound green pellets without any additional step, since it has excellent flowability. Power B, hardly be made into sound green pellets because of its poor flowability.

The O/U ratios of the sintered pellets were controlled by the following equations where the relationship of x in UO_{2+x} versus Po_2 is given by

$$\log Po_2 = A + B \log x + C (\log x)^2 \quad (1)^{(11)}$$

$$A = -33.602 + 40.842 \times 10^{-3} T - 12.615 \times 10^{-6} T^2 \quad (1\text{-}a)$$

$$B = -9.983 + 18.021 \times 10^{-3} T - 5.387 \times 10^{-6} T^{-2} \cdots (1\text{-}b)$$

$$C = -3.366 + 5.011 \times 10^{-3} T - 1.478 \times 10^{-6} T^{-2} \cdots (1\text{-}c)$$

where T is in °C and Po_2 in atmosphere.

From the oxygen partial pressure, the ratio of CO_2/CO can be determined from the free energy equation,

$$\log (CO_2/CO) = \frac{14,757}{T(°K)} - 4.528 - \frac{1}{2} \log Po_2 \quad (2)^{(18)}$$

Both CO_2 and CO gases were dried with conc-H_2SO_4, silicagel and $CaCl_2$ before mixing the gas streams. The mixed gas passed through capillary flowmeters to the sintering furnace at the rate of 200ml/min during the whole cycle.

The specimens initially placed at the central heating zone of the furnace tube, and atmosphere was replaced with nitrogen before heating, then the CO_2/CO mixed gas was introduced into the furnace before heating.

The specimens were heated at the rate of 7°C/min from the ambient temperature to the sintering temperature which was measured and controlled with the thermocouple located at the central heating zone. Throughout the the heating cycle, the stoichiometry of the uranium oxide was fixed by flowing the appropriate CO_2/CO gas mixture continuously over the specimen.

The progress of densification of the compacts

of $UO_{2.005}$, $UO_{2.01}$, $UO_{2.04}$ and $UO_{2.10}$ was studied in the temperature range of 1000°C to 1200°C for 30 to 600 minutes. At the end of the sintering period, the specimen was cooled by brining it slowly to the cold end zone of the furnace tube surrounded by a water jacket.

The results of sintering were evaluated by measuring the density of each specimen with immersion method. The mean grain size was determined with the linear intercept method and the pore size was analyzed with OPTMAX Image Analyzer from the metallograph of microstructure. The O/U ratio of sintered pellet was measured with the oxidation-reduction method.

3. Result and Discussion

3-1. Desification and grain growth

In order to compare the sinterability of powder A and B, these powders were compacted and sintered for $UO_{2.10}$ at 1200°C which was the highest O/U ratio and temperature of the present study, and the sintered results revealed as shown in fig. 2.

A value of over 96% T.D. was obtained by sintering for 1 hour with the compacts of powder A, however, powder B was reached only 93% T.D. even being sintered longer than 4 hours. Microstructures and pore distributions sintered specimens of powder A and powder B

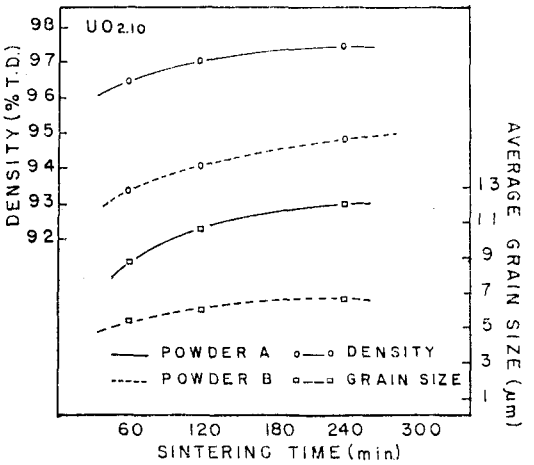

Fig. 2. Sintered Density and Grain Size vs. Sintering Time for Isothermal Sintering of Powder A and B.

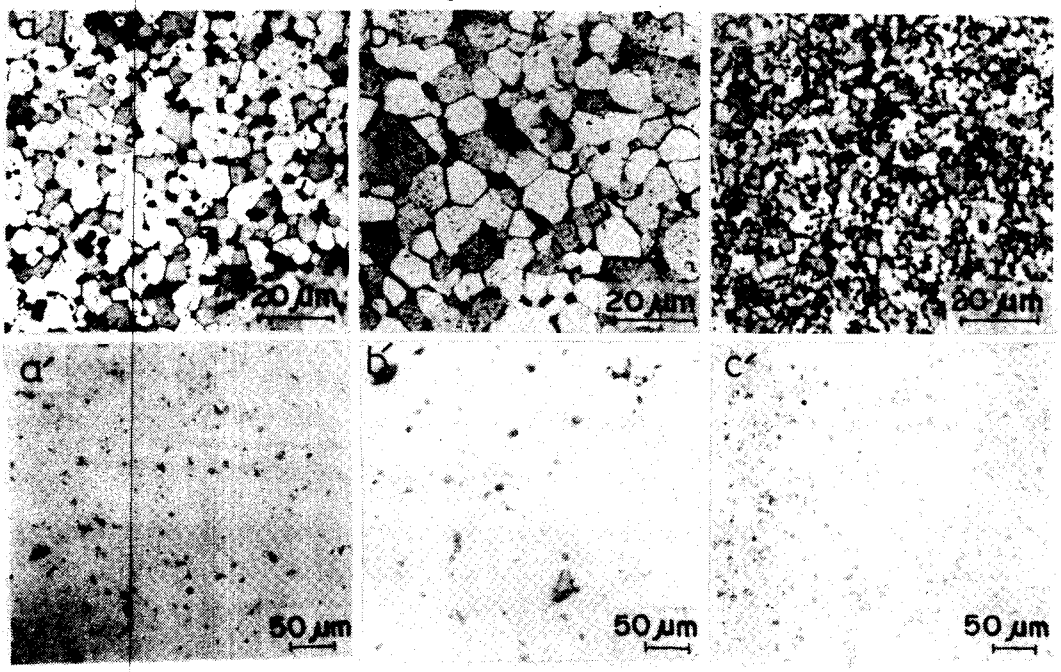

Fig. 3. Microstructual Grain and Pore of The Sintered Pellets of $UO_{2.005}$, Sintered at 1,200°C for 30min. (a.a'), 240min. (b,b') Powder A, and 240min (c,c') Powder B.

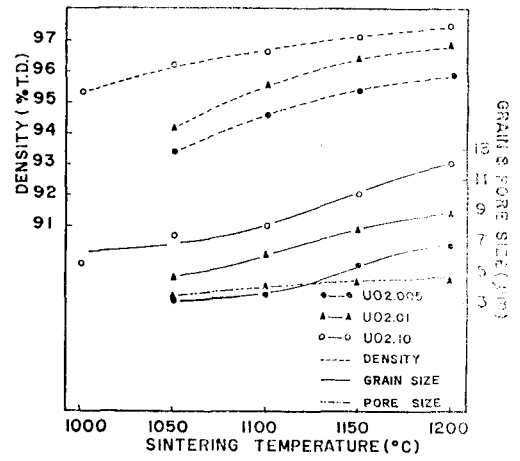

Fig. 4. Variation in Sintered Density and Average Grain Size of Sintered Pellet With Sinter ing Temperature after Sintering for 240min.

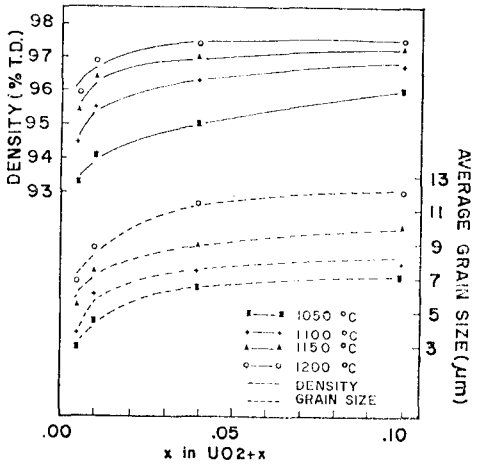

Fig. 5. Density and Average Grain Size of Sintered Pellets vs. X in UO_{2+x} after Isothermal Sintering for 240min.

are shown in fig. 3. A distinct grain and pore growth of powder A were observed by sintering at 1200°C withinerease of time for $UO_{2.005}$ as shown in a, a′, b and b′, of the figure. From c and c′ of fig. 3, it is hardly to notice the grain and pore growth of the sintered $UO_{2.005}$ of powder B at 1200°C for 4 hours. The present work, therefore, only dealt with powder A here after.

The changes of the density, grain size and pore size of sintered powder A compacts after sintering for 240 minutes are shown in fig. 4 and 5 as a function of sintering temperature and x of UO_{2+x}. The density and grain size of sintered UO_{2+x} compact was increased with increasing x and sintering temperature, but the pore size did not change so much with increasing sintering temperature. The *sinterability* of the compacts enhanced suddenly with a small increasing of x ($x=0.005\sim0.04$) in near hyperstoichiometric composition of UO_2 comparing to the higher hyperstoichiometric composition $x\geq0.04$. It is apparent from the curves that consistent densities above 95% T.D. can be reached very easily at relatively low temperature for powder A of $UO_{2.10}$ at 1000°C, $UO_{2.01}$ at 1100°C and $UO_{2.005}$ at 1150°C.

The variation of oxygen partial pressure and sintering temperature generated microstructual changes of sintered pellets as shown in fig. 6. From (a), (b) and (c) of the figure, a distinct difference of grain size and its distribution was observed due to only small variation of the O/U ratio at a constant sintering temperature and period. A discontinuous grain growth was revealed at the higher O/U ratio and temperature as shown in fig. 6—(c) and—(d). Consequently most of the pores, which located initially at the grain boundary, were entraped to the discontinuously grown grains. This discontinuous grain growth started from when the average grain size became 8 μm. The temperature and time for sintering, which yields discontinuous grain growth, decreased with increasing O/U ratio and a reciprocal relationship is revealed between the temperature and time as shown in fig. 7. This discontinuous growing phenomena could not be explained definitely at present work, it, however, might be attributed to the same cause as secondary recrystallization process.

The values of densification parameter of powder A are illustrated as a function of time for

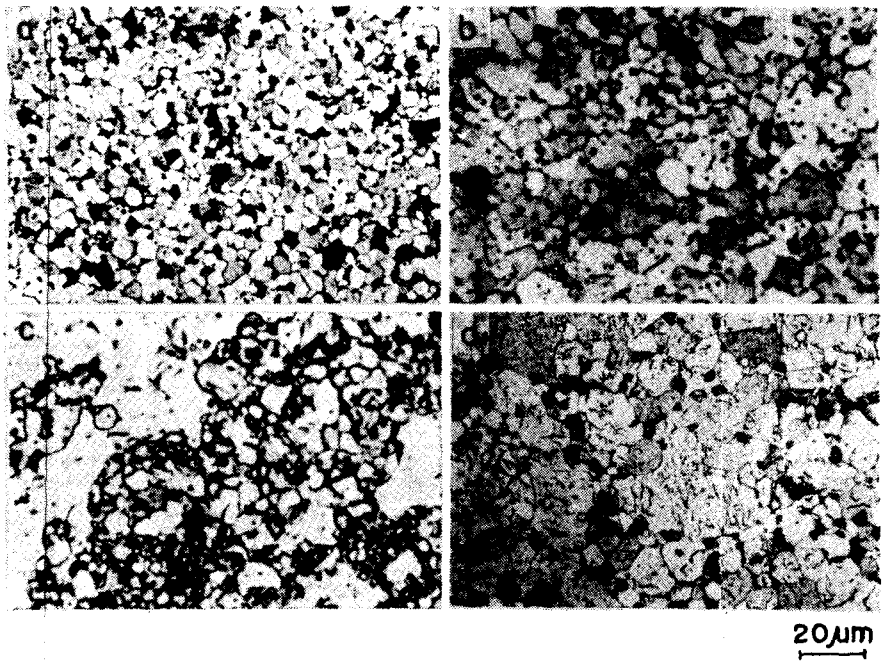

Fig. 6. Metallographs of The Sintered Pellets of a) $UO_{2.005}$, b) $UO_{2.01}$ and c) $UO_{2.10}$ at 1100°C and d) $UO_{2.10}$ at 1200°C for 4 hr.

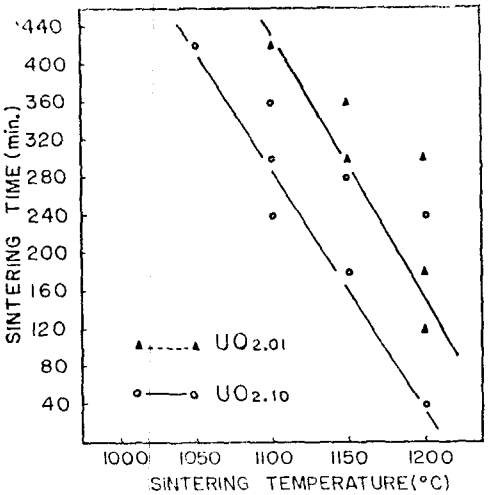

Fig. 7. Sintering Time vs. Temperature for Discontinuous Grain Growth of $UO_{2.01}$ and $UO_{2.10}$.

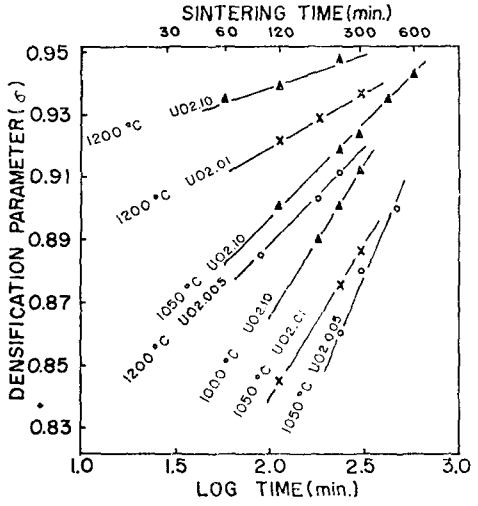

Fig. 8. Densification Parameter vs. Sintering Time for Different O/U Ratios.

the various temperature and O/U ratios in fig. 8. The desification parameter, σ is defined as

$$\sigma=\frac{\text{sintesred density}-\text{green density}}{\text{theoretical density}-\text{green density}}$$

The linear time dependence of densification shows that the densification is a simple reactions involving a single atomic process. The slope of densification parameter vs. log(time) decreased with increasing the O/U ratio from 2.005 to 2.10 at constant temperature and increasing the sintering temperature at the constant O/U ratio. The relatively rapid decrease of slope of

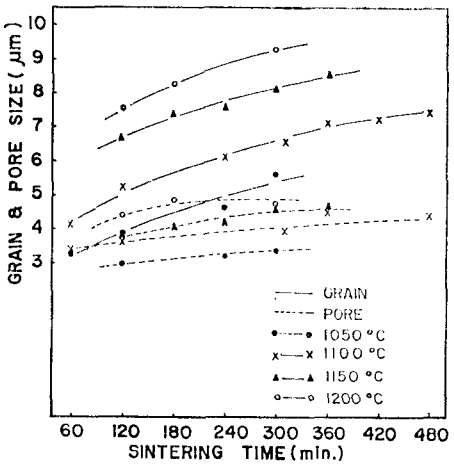

Fig. 9. Change in Average Grain Size and Pore size with Sinting Time at Various Temperature.

the densification parameter versus log (time) curve at 1200°C and 1050°C in $UO_{2.10}$ reveals the decreasing of the densification effects at the stage of discontinuous grain growth.

As shown in fig. 9, the grain size of sintered pellet increased with sintering time, however the increasing tendency of the average pore size slowed down, and at last no increase of pore size was revealed at 1200°C after 180 minutes of isothermal sintering.

3-2. Sintering Diagram

The sintering rate of pure stoichiometric UO_2 is usually controlled by sintering temperature and time in the case of using the same powder and atmosphere. However, in the present study, the stoichiometry of UO_2 was changed by intr-oducing a slightly oxidative gas atmosphere produced by changing mixing ratio of CO_2/CO, and the sinterability of uranium dioxide revealed quite different results depending on the oxygen partial pressure in the atmosphere then on the O/U ratio of the pellet.

In the practical point of view, it is necessary to establish a diagram showing the relation of the temperature-time-density-grain size for the sintering of nonstoichiometric uranium dioxide pellets. Using the data of present study, such a diagram was established for each O/U ratio as fig. 10 and fig. 11.

For example, in the case of the O/U ratio of 2.01, density of 96% T·D. and grain size of 7μm could be obtained after sintering at 1200°C for 30 minutes, at 1150°C for 180 minutes and at 1100°C for 360 minutes, respectively, as shown in fig. 11. From these diagrams and equation (2), the important nuclear specifications of the pellet; i.e. density 95% T.D., O/U$\leq$ 2.01, grain size=5−25μm could be achieved with oxidative sintering which carried out in an atomosphere of controlled CO_2/CO ratio and at

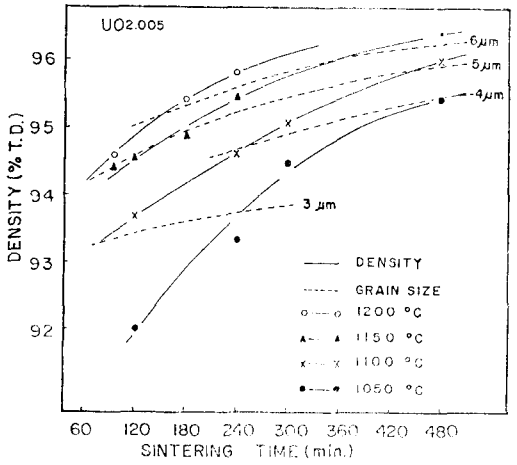

Fig. 10. Sintering Diagram for $UO_{2.005}$.

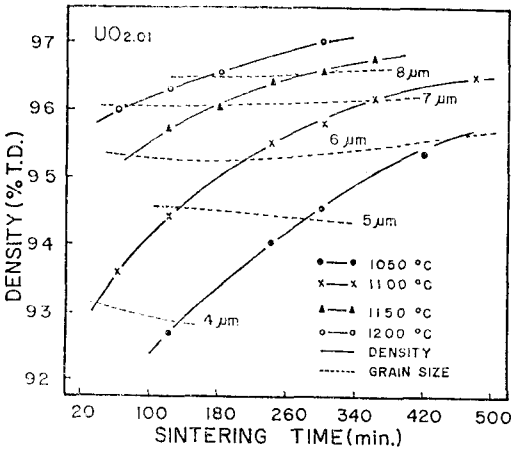

Fig. 11. Sintering Diagram for $UO_{2.01}$.

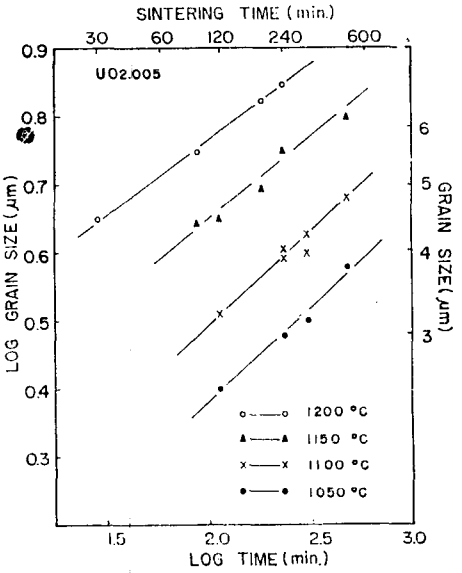

Fig. 12. Grain Size vs. Sintering Time of Isothermally Sintered $UO_{2\cdot005}$ Pellet.

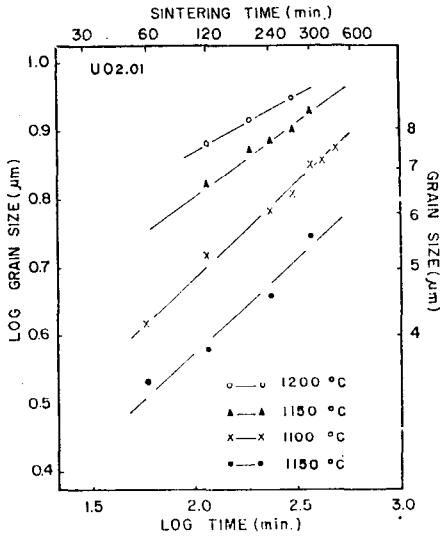

Fig. 13. Grain Size vs. Sintering Time Isothermally Sintered $UO_{2\cdot01}$ Pellet.

temperature lower 500~600°C than conventional sintering process.

3-3. Activation energy at the final stage sintering

In order to examine whether grain growth during the sintering of UO_2 could be expressed by an empirical equation, the average grain size of sintered pellet was plotted with sintering time on logarithmic scales at different temperatures as shown in fig. 12 and 13.

The plots of the data for $UO_{2.005}$ for the respective isotherms constituted nearly the same slopes of 0.25 in the sintering temperature range of 1050°C to 1200°C. In the case of $UO_{2.01}$ also exhibited the same value of 0.25 as the slope below 1150°C, however, at 1200°C the slope declined to 0.19 as shown in fig. 13.

The relatioship between grain size and sintering time fitted to the form of an empirical equation, $D=(Kt)^n$,[19,20,21] where D is the average grain size, K: rate constant, n: slope, t: soaking time in minutes. A value of 0.25 could be taken as the parameter of n in the relation of $D=(Kt)^n$.

Using Oswald ripening theory, Hillett proposed a relationship of $D=t^{1/3}$(22) for sintering ceramics, which contains inclusion. The grain growth of the present study obeyed the relationship of $D=(Kt)^{1/4}$ in the range of normal continuous grain growth of sintering stage. When discontinuous grain growth happened, the average grain growth rate was suppressed and the relation was changed and revealed as $D=(Kt)^{1/5}$.

The rate constant, K, of the above relation contains the factor of grain boundary mobility, which depends on temperature by Arrhenius equation, hence the rate constant may be expressed as $K=A\exp(-Q/RT)$,[21] where, Q is the activation energy in cal/mole, R, gas constant, T, absolute temperature. Thus, the grain size-time relation is reformed in the equation of $\log K=\frac{1}{n}\log D-\log t=-\frac{Q}{2.303T}+\log A$.

In the present study, the progress of sintering was measured by grain size. Consequently, to see whether the sintering of final stage may be regarded as a single rate process, it is necessary to plot curves of constant grain size D on a

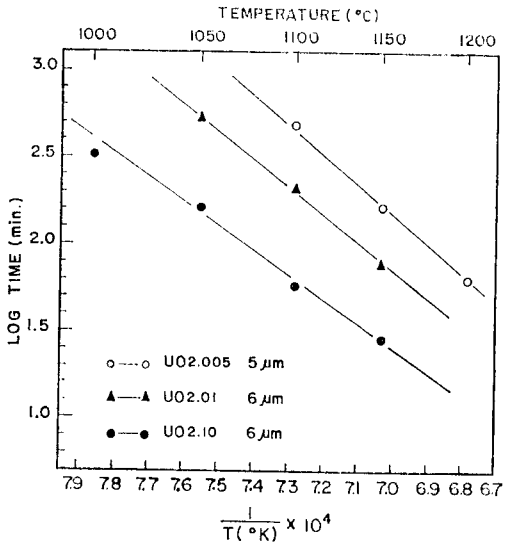

Fig. 14. Relation between Sintering Time and Reciprocal Temperature to Obtain an Average Grain Size in $UO_{2\cdot005}$, $UO_{2\cdot01}$, $UO_{2\cdot10}$.

graph of log t vs. $1/T$, if the above relation is satisfied, the plot should be drawn in a straight line. The plot of constant D in fig. 14 established straight lines for $UO_{2.005}$, $UO_{2.01}$ and $UO_{2.10}$. The values of Q obtained from fig. 14 are 75±3, 64±4 and 62±3 kcal/mole in O/U ratios of 2.005, 2.01 and 2.10 respectively.

The initial stage sintering behavior of hyperstoichiometric UO_{2+x} has been studied by many researchers. And the activation energies measured from shrinkage kinetics were reported to be the values of wide range, i.e. 40kcal[7]/mole (in CO_2 atmosphere), 55[8]kcal/mole ($UO_{2\cdot008}$), 53[9]kcal/mole ($2.003 \leq O/U \leq 2.14$), 65.8[10] kcal/mole ($2.06 \leq O/U \leq 2.49$) and 107[11]kcal/mole ($UO_{2.02}$). This variation could be caused from the differences of powder properties, sintering temperature and atmosphere and experimental error etc, between each works.

For the activation energy of the final sintering stage, a value of 120.3[23] kcal/mole was reported by an experiment of isothermal grain growth kinetics in high temperature sintering of stoichiometric UO_2.

The values of the lower activation energies, such as 40 kcal/mole,[7] 55[8] and 53[9] kcal/mole, were attributed to the grain boundary diffusion, and the higher values and later stage of sintering were deduced to volume diffusion.

The activation energy of the present study for sintering of hyperstoichiometric uranium oxide is equivalent with the values of Alcock[24] and Yajima.[25] Therefore, the volume diffusion could be regarded as the controlling mechanism of the final sintering stage of UO_{2+x}.

while the activation energies of the present study exhibited a little decrease, however, the sinterability was remarkably enhanced with increasing $\times$ in UO_{2+x}. Excess oxygen ion diffused into the lattice would increase with $\times$ and then increase the introduction of vacancies into the uranium lattice, and the excess concentration of vacancy would increase the frequency factor of the diffusion coefficient of the uranium ions. Therefore, the increased sinterability with $\times$ in UO_{2+x} could be mainly deduced to the increase of the frequency factor of the uranium diffusion coefficient.

Conclusions

1) Some of the requested specification for nuclear fuel pellet; the density $\geq$ 95% T.D., the average grain size $\geq 7\mu$m, and $O/U \leq 2.01$; were obtained in a single step oxidative sintering by adjusting CO_2/CO ratio of the atmosphere in the range of temperature 1100°C~1150°C.

2) The specification of the pellet could be adjusted using the diagram showing the relation of the temperature-time-density-grain size for hyperstoichiometric uranium oxide sintering.

3) Continuous growth rate of the sintered UO_{2+x} followed the expirical equation of $D=(Kt)^{\frac{1}{4}}$ when isothermally sintered under the mixed gas atmosphere of CO_2/CO.

4) The activation energies for the grain growth in the final stage of sintering decreased a little with increasing x; the values are 75 ± 3, 64 ± 4 and 62 ± 3 kcal/mol in O/U ratio of 2.005, 2.01 and 2.10 respectively. These values correspond to the energy for volume diffusion.

Acknowledgement

The authors wish to acknowledge the members of Fuel Fabrication Division and QC Division, KAERI, for their assistance in sample preparation and analysis, also wish to thank the Asan Welfare Foundation for the research subsidy.

Reference

1. H.J. Matzke, *J. Nucl. Mat.*, **20**, 328(1966).
2. B.E. Schaner, *Am. Cerm. Soc. Bull.*, **38**, 494 (1959).
3. M. El-Sayed Ali and R. Lorenzelli, *J. Nucl. Mat.*, **87**, 90(1979).
4. W.I. Stuart and R.B. Adams, J. Nucl. Mat., **58**, 201(1975).
5. W.E. Baily, J.C. Danko, and H.H. Ferrari, *J. Am. Ceram. Bull.*, **41**, 768(1962).
6. W. Dörr and H. Assmann, CIMTEC, May 28-31 (1979).
7. I. Amato, R.L. Colombo and A.M. Protti, *Nucl. Sci. Eng.*, **16**, 137(1963).
8. K.W. Lay, *J. Am. Ceram. Soc.*, **54**, 18(1971).
9. M.J. Bannister and W.J. Buykx, *J. Nucl. Mat.*, **64**, 57(1977).
10. I. Amato, R.L. Colombo and A.M. Protti, *J. Nucl. Mat.*, **11**, 229(1964).
11. K.W. Lay and R.E. Carter, *J. Nucl. Mat.*, **30**, 74(1969).
12. Boon Wong and Joseph A. Pask, *J. Am. Cerm. Soc.*, **62**, 138(1979).
13. D.L. Johnson and I.B. Cutler, *J. Am. Ceram. Soc.*, **46**, 541(1963).
14. H. Lchinose and G.C. Kuczynski, *Acta Met.*, **10**, 209(1962).
15. R.L. Eadie, D.S. Wilkinson and G.C. Weatherley, *Acta Met.*, **22**, 1185(1974).
16. Sven. G. Brandberg, *Nucl. Tech.*, **18**, 177(1973).
17. H. Doi and T. Ito, *J. Nucl. Mat.*, **11**, 94(1964).
18. K. Hagemark and M. Broli, *J. Inorg. Nucl. Chem.*, **28**, 2837 (1966).
19. W.D. Kingery and B. Francois, *J. Am. Cer. Soc.*, **48**, 546(1965).
20. J.E. Burke, Technical Information Series, 68-C-368 (1968).
21. H.J. Hamjian and W.G. Lidman, Trans. AIME, **197**, 696(1953).
22. M. Hillert, *Acta Met*, **13**, 227(1965).
23. R.N. Singh, *J. Nucl. Mat.*, **64**, 174(1977).
24. G.B. Alcock, R.J. Hawkins, A.W.D. Hills, and P. McNamara, Paper SM-66/36, IAEA Symp. Thermodynamics (Vienna, 1965).
25. S. Yajima, H. Furuya and T. Hiroi, *J. Nucl. Mat.*, **20**, 162(1966)